Cellular and Molecular Bioengineering, Vol. 8, No. 2, June 2015 (© 2015) pp. 247–257
DOI: 10.1007/s12195-015-0383-x

Collective Migration Exhibits Greater Sensitivity But Slower Dynamics of Alignment to Applied Electric Fields

MARK L. LALLI[1] and ANAND R. ASTHAGIRI[1,2]

[1]Department of Chemical Engineering, Northeastern University, 360 Huntington Ave., Boston, MA 02115, USA; and [2]Department of Bioengineering, Northeastern University, Boston, MA 02115, USA

(*Received 16 December 2014; accepted 28 February 2015; published online 8 March 2015*)

Associate Editor Jason M. Haugh oversaw the review of this article.

Abstract—During development and disease, cells migrate collectively in response to gradients in physical, chemical and electrical cues. Despite its physiological significance and potential therapeutic applications, electrotactic collective cell movement is relatively less well understood. Here, we analyze the combined effect of intercellular interactions and electric fields on the directional migration of non-transformed mammary epithelial cells, MCF-10A. Our data show that clustered cells exhibit greater sensitivity to applied electric fields but align more slowly than isolated cells. Clustered cells achieve half-maximal directedness with an electric field that is 50% weaker than that required by isolated cells; however, clustered cells take ~2–4 fold longer to align. This trade-off in greater sensitivity and slower dynamics correlates with the slower speed and intrinsic directedness of collective movement even in the absence of an electric field. Whereas isolated cells exhibit a persistent random walk, the trajectories of clustered cells are more ballistic as evidenced by the superlinear dependence of their mean square displacement on time. Thus, intrinsically-directed, slower clustered cells take longer to redirect and align with an electric field. These findings help to define the operating space and the engineering trade-offs for using electric fields to affect cell movement in biomedical applications.

Keywords—Cell–cell interactions, Directional bias, Electrotaxis, Persistence.

INTRODUCTION

Extracellular electric fields are commonly found within the body in both healthy and diseased tissue. Transepithelial potentials (TEPs) on the order of tens of millivolts have been measured in tissues, such as skin, breast and prostate ducts.[8,11,26] Larger potentials on the order of hundreds of millivolts are generated by the flow of blood through the human circulatory system.[2] Rapid cell growth and associated significant alterations in surface charges induces an electric field between the tumor environment and regions of healthy tissue adjacent to it.[6]

These extracellular electric fields play an important role in physiological processes. It is well known that reorientation and extension of neuron processes are influenced by electric fields.[25] Meanwhile, wounds in tissues, such as the skin, compromise the TEP and produce an ionic current, providing a stimulus for directed cell migration to close the wound.[41] For example, currents of up to 1 μA/mm of wound perimeter and electric fields of up to 2 V/cm were observed in wounds of skin epithelium.[11] In fact, imposing an opposing electric field is sufficient to overwhelm other stimuli and reverse wound closure, with cells migrating away from the wound edge.[27,40,41] The alignment of cell migration within externally applied electric fields, known as electrotaxis, has been reported in a number of cell systems, including fibroblasts, endothelial cells and normal and cancerous epithelial cells.[13,20,21,32,35,39]

For tissues such as the epithelium and endothelium, understanding electrotaxis particularly in the context of collective movement is important. Directed collective migration plays an important role in processes such as wound healing, angiogenesis and the metastasis of cancer cells away from the primary tumor.[4,5,17,28,36] Geometric confinement, substrate stiffness and other microenvironmental parameters are known to affect the ability and efficiency of collective movement.[24,29,37] With electric fields already being applied in clinical applications, such as drug delivery, hyperthermic eradication of tumors, spinal cord regrowth, and ulcer healing,[12,15,18,30] it is essential to understand the effect of electric fields on cell migration in surrounding tissues where cell–cell interactions are prevalent. Furthermore, a quantitative understanding of the effect of

Address correspondence to Anand R. Asthagiri, Department of Chemical Engineering, Northeastern University, 360 Huntington Ave., Boston, MA 02115, USA. Electronic mail: a.asthagiri@neu.edu

electric field on the dynamics of collective migration would offer insights into utilizing this microenvironmental property to tune multicellular rearrangements in applications such as tissue engineering.

Collective movement is fundamentally different from the migration of isolated cells. Migration within a cluster requires the maintenance of intercellular adhesions and cell–cell signaling complexes. During collective migration, cell–cell adhesions allow for mechanotransduction and the propagation of correlated movement.[14,24] Likewise, gap junctions within an epithelial layer mediate direct intercellular exchange of second messengers, particularly relevant to electric fields as they affect the distribution of calcium and other ions.[1,23] Furthermore, the movement of clustered cells may be contact-inhibited and constrained by the lack of space to extend protrusions.[22] While both isolated and clustered cells remodel the underlying matrix and produce and consume growth factors,[33] these processes are likely to be significantly different in the two situations due to differential ligand processing at the higher local density of cells in a cluster and due to the effect of cell–cell interactions on the distribution of forces that act on and help to remodel the matrix.

Given the complexity of collective movement, it is unclear how an electric field will affect collective migration and how this effect will differ from the response of isolated cells. In this study, we examine this question by conducting a quantitative comparative analysis of the electrotaxis of isolated and clustered cells using the MCF-10A non-transformed human mammary epithelial cell line as a model system.

MATERIALS AND METHODS

Cell Culture

MCF-10A non-transformed human mammary epithelial cells were obtained from ATCC. Cells were cultured in growth medium composed of Dulbecco's modified Eagle's medium/Ham's F-12 containing HEPES and L-glutamine (DMEM/F12, Invitrogen) supplemented with 5% horse serum (Invitrogen), 1% penicillin/streptomycin (Invitrogen), 10 μg/mL insulin (Sigma), 0.5 μg/mL hydrocortisone (Sigma), 20 ng/mL EGF (Peprotech) and 0.1 μg/mL cholera toxin (Sigma) and were maintained under humidified conditions at 37 °C and 5% CO_2. Cells were passaged as described previously[16] and were discarded after passage 35.

Device Fabrication

The electrotactic chamber was assembled similar to that described and validated by Song.[31] Briefly, polystyrene dishes (60 mm) were taken and marked with lines 12 mm apart. Number 1 glass coverslips (22×22 mm^2) were cut in half and then attached to either side of the lines using DC4 silicon grease (Dow Corning), leaving a 12 mm gap between them to produce a 12 mm × 22 mm cell seeding region on the dish. Barriers were constructed orthogonally from the edge of the glass coverslips using 3140 silicon adhesive (Dow Corning) in order to produce two media reservoirs on either side of the 12 mm × 22 mm gap. Dishes were then left to dry for at least 12 h while being sterilized under ultraviolet light and were then stored for up to 4 weeks.

Polydimethylsiloxane (PDMS) was synthesized by mixing prepolymer to cross-linker in a 10:1 ratio. In order to remove air bubbles from the mixture, and therefore from the finished product, the solution was degassed in a vacuum chamber until expulsion of bubbles ceases. The mixture was then cured at 80 °C for 1 h in an unmodified plastic dish (100 mm diameter). Wells were cut from PDMS blocks so as to fit onto the gap between the coverslips and sterilized.

Dishes were then coated with a 10 μg/mL solution of fibronectin (Invitrogen) in PBS (Invitrogen) for 1 h prior to cell seeding. Cell solution (500 μL) was seeded into the PDMS well placed between the coverslips at varying concentrations (~10^3–10^5 cells/mL) and left to adhere for at least 12 h in incubation. After rinsing with growth media to removed non-adherent cells, a coverslip roof was attached to the chamber *via* DC4 silicon grease in order define a chamber with dimensions 12 mm × 22 mm × 0.15 mm. After closing the chamber, media was replenished once more before imaging.

Image Acquisition

Imaging was performed on an AxioVert 200 M inverted microscope (Zeiss). Devices were maintained at 37 °C and 5% CO_2 for 6 h. Current was delivered to the chamber *via* two agar bridges (6″ × 7 mm ID) which were bent under flame to fit beneath the condenser of the microscope. The agar bridges were comprised of a 5% w/v solution of agarose (EMD) dissolved in heated serum free media and left to cool and solidify at 37 °C. The use of serum free media in the agar bridges was found to help stabilize the pH of the media throughout the 6 h experimental window. Current was generated by a WaveNowXV potentiostat (Pine) connected to disposable aluminum electrodes resting in reservoirs of 1 M KCl solution. KCl reservoirs were kept at approximately equal liquid height as the media in the device to prevent syphoning of fluid. After 6 h, no syphoning of KCl into device media was observed. Phase images were taken every 5 min.

Image Analysis and Quantification of Cell Migration

Time lapse images were processed using a custom tracking interface written in MATLAB (MathWorks, Natick, MA) in order to extract the two-dimensional position of cells with respect to time and store them in Excel. Cells were manually selected in the initial frame of reference for each video and were subsequently tracked individually with the user specifying the cell center. Cells which divided during the middle of the video were discarded, as well as cells which died, detached from the substrate, or were otherwise compromised. In the case of isolated cells, colliding/attaching with another cell also led to discarding. Cells which left the field of vision were tracked until that time, and positional data from time 0 to t, where $t < 6$ h, was compiled with the remainder of the data.

Cell trajectories were analyzed further using MATLAB to assess several properties of migration.

Directedness (D) was calculated using Eq. (1),

$$D = cos(\theta) \tag{1}$$

where θ is the angle between the electric field (black vector shown in Fig. 1) and the cell displacement (red vector shown in Fig. 1). By this definition, a directedness value of 1 or -1 would be indicative of a net directional bias toward the anode or the cathode, respectively.

Persistence was calculated from Eq. (2),

$$P = x/l \tag{2}$$

where l is the path length of a cell (blue line shown in Fig. 1) and x is the net displacement over the same amount of time. The additive predicted persistence of clustered cells (P^*) was calculated by Eq. (3),

$$P^*|_E = P_{\text{isolated}}|_E + (P_{\text{clustered}} - P_{\text{isolated}})|_{E=0} \tag{3}$$

where E is the electric field strength and P_{isolated} and $P_{\text{clustered}}$ are the measured values of persistence of the isolated and clustered cells, respectively. The error in P^* was computed by the propagation of errors and is equal to the sum of the errors associated with each term that contributes to the value of P^*.

Mean square displacement (MSD) was calculated from Eq. (4),

$$MSD(\Delta t) = \sum_{c=1}^{n} x(\Delta t, c)^2 \tag{4}$$

where $x(\Delta t, c)$ represents the displacement of a cell between its position at time, t, and $t + \Delta t$ for case, c. n is the number of possible cases for which the displacement at Δt can be calculated. For example, 12 cases of $\Delta t = 5$ min exist per cell in a 1 h long time lapse. Therefore, n would equal the sample size of cells multiplied by 12.

The MSD curves were then plotted and fitted to Eq. (5) using MATLAB's nlinfit command in order to calculate the exponent of the function,

$$MSD = \alpha t^{\beta} \tag{5}$$

where t is the time difference between two points and α and β are calculated coefficients.

The evolution of directedness, $D(t)$, for cells initially moving in the direction opposite to the expected long term direction was fit to the following exponential recovery model using MATLAB's nlinfit:

$$D(t) = (D_{\text{ss}} - D_{\text{min}})\left(1 - e^{-\lambda t}\right) + D_{\text{min}} \tag{6}$$

where D_{ss} is the upper asymptote (steady-state value) of the curve, D_{min} is the nadir of the curve, λ is recovery coefficient (min^{-1}), and t is the time (min). The characteristic time needed to reach half maximal recovery (τ) is related to the recovery coefficient by the following equation:

$$\tau = \log(2)/\lambda \tag{7}$$

RESULTS

Clustered MCF-10A Cells are More Sensitive to Electric Potential than Isolated Counterparts

To investigate collective movement in an electric field, the trajectory of isolated and clustered MCF-10A cells were observed by time-lapse microscopy in the absence of an electric field or in the presence of different electric field strengths. In the presence of an electric field of 1.0 V/cm, both isolated and clustered cells were observed to migrate toward the anode (Fig. 2a and Supplemental Videos 1–2). Meanwhile, in the absence of an electric field, there was no apparent directional bias in the movement of the cells (Supplemental Videos 3–4). Visualizing the trajectory of twenty randomly selected cells qualitatively confirmed the electrotactic movement of both isolated and clustered MCF-10A cells (Fig. 2b). Interestingly, from this small sample of trajectories, isolated cells appeared to require an electric field strength of 0.51 V/cm to direct their migration toward the anode; in contrast, clustered cells seemed to exhibit directed migration within a weaker electric field of 0.26 V/cm.

To investigate more quantitatively whether isolated and clustered cells have different sensitivity to electric field strength, we quantified the trajectories of approximately 2500 isolated and 7000 clustered cells across five levels of electric field. We determined the percentage of cells migrating toward the anode of the electric field: cells whose final position was closer to the anode than their initial position were scored as having

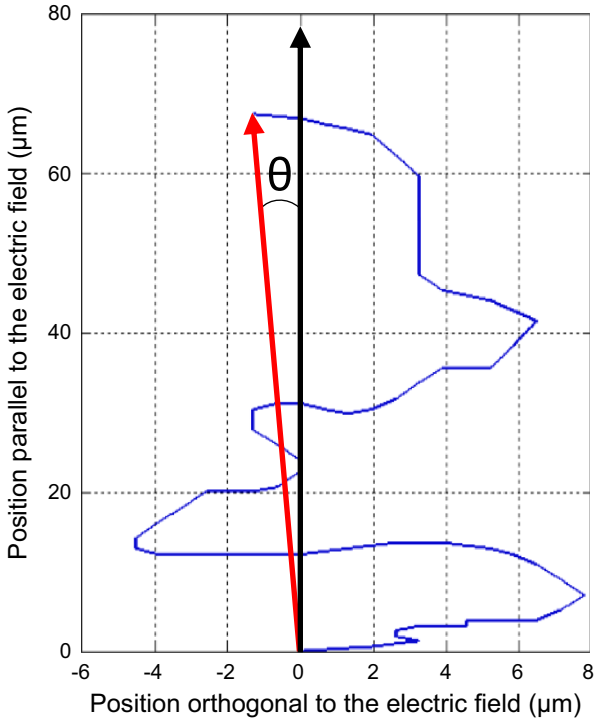

FIGURE 1. A schematic of the trajectory of a cell migrating within an electric field. The black line indicates the electric field vector from cathode to anode and the blue line shows the trajectory of the cell in time. The red line represents the overall displacement of the cell. The angle between the electric field vector and the cell displacement vector is labeled θ.

migrated toward the anode (Table 1). Cluster size ranged from dozens of cells to hundreds of cells reaching partial confluence. Even at the lowest applied electric field of 0.13 V/cm, a much larger fraction of clustered cells moved toward the anode in comparison to isolated cells. Meanwhile, under control conditions in the absence of an electric field, both isolated and clustered cells showed no appreciable bias toward the anode.

To gauge the extent to which cell movement is aligned with the electric field, we quantified the directedness as the cosine of the angle between the cell displacement vector and the axis of the electric field (see "Materials and Methods"). A directedness value of 1 or -1 would be indicative of a net directional bias toward the anode or the cathode, respectively.

Our measurements show that for a particular magnitude of electric field, clustered cells become more aligned than isolated cells within the 6 h observation window (Fig. 3). In addition, we observe a change in the threshold required to initiate an electrotactic response. The lowest applied electric field (0.13 V/cm) is sufficient to increase the directedness of clustered cells above the baseline control case where no electric field is presented as indicated by a two-tailed t test comparing the distributions of directedness in each case ($p < 0.01$). In contrast, isolated cells require an electric field of 0.26 V/cm or greater in order to shift from their baseline response ($p < 0.01$). A weaker electric field of 0.13 V/cm is insufficient to induce directedness of isolated cells ($p > 0.01$).

To examine the directedness of cells at a single-cell level, we constructed circular histograms (rose plots) of the angle between the vector of displacement after the observation window and the axis of the electric field (Fig. 4). Using the omnibus test in the Circular Statistics Toolbox for MATLAB,[3] we tested the null hypothesis that the distribution of angles is uniform. Among isolated cells exposed to an electric field, the null hypothesis was rejected for electric fields at or above 0.26 V/cm ($p < 0.01$) but not at 0.13 V/cm, further confirming that a potential gradient greater than 0.13 V/cm is needed to induce electrotaxis of isolated cells. In contrast, the rose plot for clustered cells scored as nonuniform at all applied electric fields. The v test confirmed that the directional bias is indeed toward zero degrees, the direction of the anode, in all cases for which the omnibus test rejected the null hypothesis. These results show that clustered MCF-10A cells are indeed more sensitive to an electric field than isolated cells, consistent with similar enhanced sensitivity of clustered MDCK I and MDCK II cells reported previously.[19]

Interestingly, the rose plots for clustered cells exhibited an unexpected feature in the control case where no external electric field is applied. The omnibus test revealed that the displacement direction of clustered cells was nonuniform. In contrast, isolated cells exhibited a uniform distribution of displacement angles under control conditions. Further analysis with the v test revealed that the direction of movement of clustered cells was nonuniform with a range of angles showing bias, which included 45° and 135°. These results are attributed to the fact that clustered cells initially share an orientation of movement with their neighbors which is stochastic in nature. These subgroups effectively reduce the sample size of independent angles, thus giving rise to a multi-modal distribution of displacement angles across the population.

Cell Clustering and an External Electric Field Additively Enhance Ballistic and Persistent Cell Movement

Our analysis shows that isolated cells have no directional bias in the absence of an external field and acquire directed movement toward the anode upon exposure to a suprathreshold electric field. These results suggest the hypothesis that isolated cells move in a persistent random walk in the absence of a field and

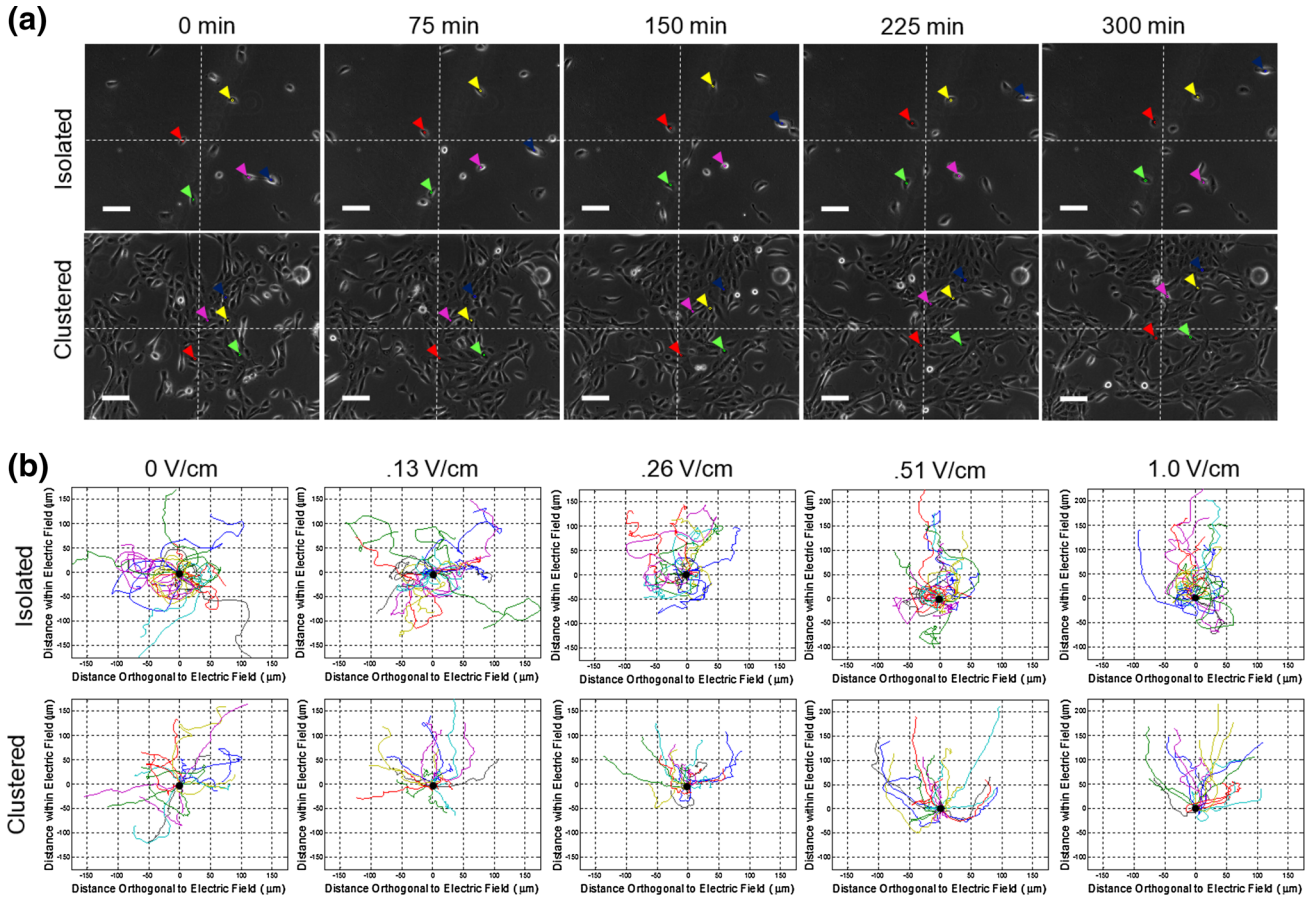

FIGURE 2. (a) Snapshots taken at times 0, 75, 150, 225, and 300 min with five isolated (top row) and clustered (bottom row) cells labeled. The white-dashed grid is centered at the same position in each image to provide a constant positional reference. Scale bar = 100 μm. The anode is in the positive y-direction. (b) Examples of 20 trajectories of isolated (top row) and clustered (bottom row) cells moving in the absence (left column) and presence of electric fields of 0.13, 0.26, 0.51, and 1.0 V/cm. A solid black circle indicates the origin (0,0) and is the starting point for every trajectory. In all cases, the anode is in the positive y-direction, and the x-direction is orthogonal to the electric field.

TABLE 1. Percentage of cells migrating[a] toward the anode of the electric field.

	Isolated cells		Clustered cells	
Electric field	% Cells aligned	Sample size[b]	% Cells aligned	Sample size[b]
0 V/cm	51.8	456	51.9	1708
0.13 V/cm	57.0	377	70.1	1491
0.26 V/cm	73.8	477	84.2	1103
0.51 V/cm	83.9	615	95.0	1550
1.0 V/cm	89.5	535	99.0	1240

[a]Cells with net displacement in the direction of the anode were scored as aligned with the field.
[b]Sample size indicates the number of cells observed over 3 independent trials.

acquire a more ballistic trajectory toward the anode upon exposure to an electric field. In contrast, our analysis demonstrates that even in the absence of an external field, subgroups of clustered cells move in a directed manner, and the external electric field acts to reorient these subgroups in the direction of the anode. Therefore, we hypothesized that clustered cells may exhibit ballistic movement even in the absence of an electric field.

Since cells with a more ballistic migration trajectory would be expected to show greater persistence, we tested this hypothesis by analyzing the persistence of clustered vs. isolated cells in the absence and presence of an electric field. Persistence was quantified as the ratio of net displacement to total distance traveled throughout the observation window (Eq. (2)). We found that the persistence of clustered cells was nearly two-fold greater than that of isolated cells in the absence of an applied electric field. The effect of applying an electric field on persistence was modest but statistically significant *via* ANOVA ($p < 0.01$). Exposure to an electric field of 0.51 V/cm and greater increased the persistence of both isolated and clustered cells (Fig. 5).

Notably, the difference in the persistence of isolated cells and that of clustered cells remained approximately constant at all electric fields, suggesting that the effects of cell clustering and the electric field on the directed migration of MCF-10A cells are additive. To examine this possibility more quantitatively, we calculated the persistence of clustered cells that would be predicted if the effect of electric field and clustering were additive (see "Materials and Methods"). The additive model predicts the persistence of clustered cells with ~ 90% accuracy (Fig. 5).

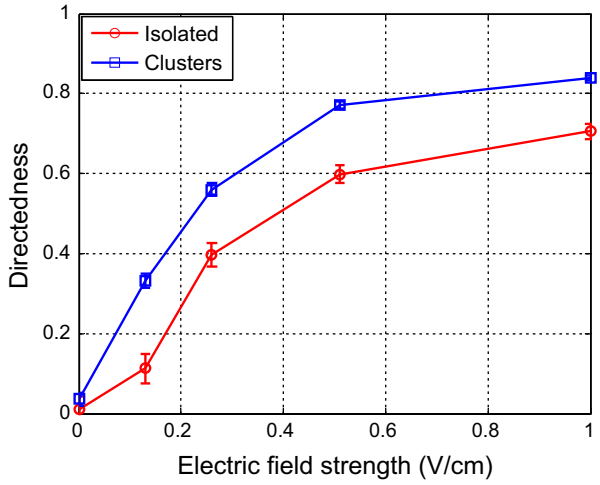

FIGURE 3. Directedness as a function of electric field. The directedness was calculated as the cosine of the angle of the final displacement vector of a cell with respect to the cathode–anode axis. The mean directedness for isolated (red) and clustered (blue) cells is depicted for electric fields of 0, 0.13, 0.26, 0.51, and 1.0 V/cm. Error bars indicate standard error of the mean.

To further characterize the ballistic vs. diffusive movement of isolated and clustered cells, we analyzed the mean square displacement (MSD) calculated from cell migration trajectories (Figs. 6a and 6b). A ballistic particle exhibits a second-order dependence of MSD on the duration of observation while the MSD will increase linearly with the time of observation for a particle undergoing Brownian motion or a random walk model of cell migration.[9] For isolated cells, we observe that the MSD increases linearly with the duration of observation in the absence of a field and for low electric fields. However, at higher field strengths (e.g., 1.0 V/cm), the dependence of MSD on duration of observation begins to exhibit some upward curvature. In contrast, for clustered cells, the curves showing the dependence of MSD on the time of observation are clearly concave upward in the absence of the electric field and for all applied electric fields. Interestingly, we see a decrease in the MSD for clustered cells (Fig. 6b) at electric fields of 0.13 and 0.26 V/cm, which corre-

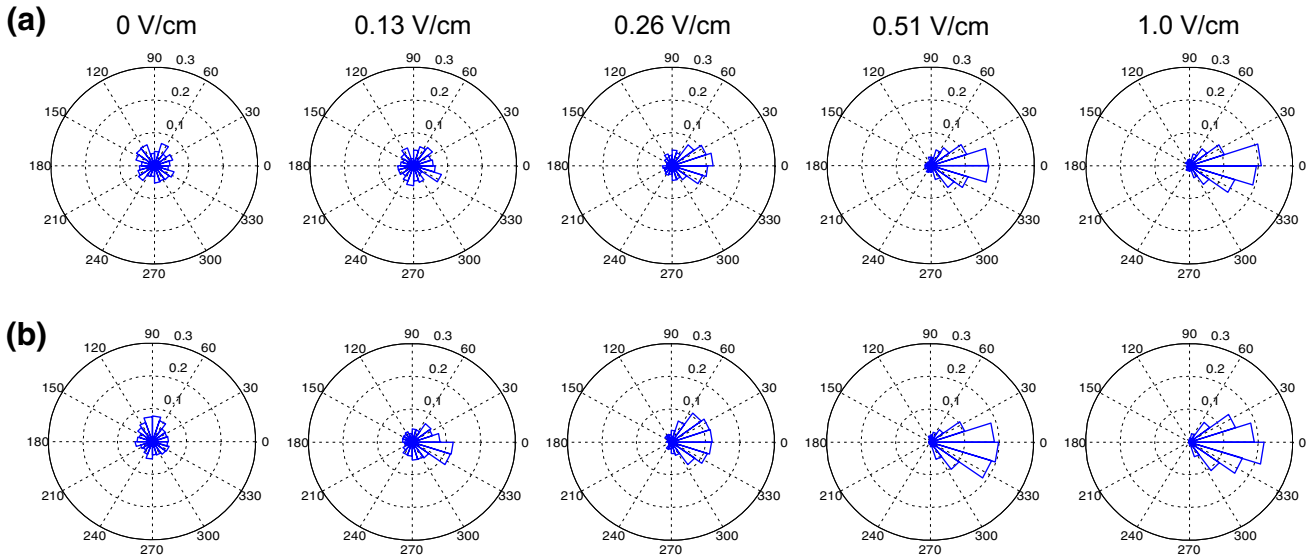

FIGURE 4. Rose plots of the angle of the displacement of isolated cells and clustered cells migrating within electric fields. (a) Rose plots of isolated cells in the absence of an electric fields (left column) or the presence of an electric field of 0.13, 0.26, 0.51, or 1.0 V/cm. The anode and cathode are at 0 and 180 degrees, respectively. In the absence of an electric field and at an electric field of 0.13 V/cm, the *p* value of the omnibus test was greater than 0.01. At all electric field strengths greater than 0.13 V/cm, the *p* value of the omnibus test was less than 0.01. These distributions also had *p* values less than 0.01 for the *v* test with selected mean of 0°. (b) Rose plots of clustered cells in the absence of an electric fields (left column) or the presence of an electric field of 0.13, 0.26, 0.51, or 1.0 V/cm. Again, the anode and cathode are at 0 and 180 degrees, respectively. At all electric field strengths greater than 0 V/cm, the *p* value of the omnibus test was less than 0.01. These also had *p* values less than 0.01 for the *v* test with selected mean of 0°. At 0 V/cm, there was a significant difference between the observed distribution and a uniform distribution although when analyzed with the *v* test, the null hypothesis could be rejected for a range of angles which included 15°, 45°, 90°, and 135°.

sponds to an observed 20% decrease in the average speed of the cells (Fig. 6c). The speed is then recovered at higher electric fields, reflected in the increase of MSD for electric fields of 0.51 and 1.0 V/cm. Notably, the speed of isolated cells is approximately twice the speed of clustered cells for all values of the electric field.

In order to characterize the extent to which the migration path was diffusive vs. ballistic, independent of cell speed, the dependence of MSD on the time of observation was fitted to a power law curve (Eq. (5)) and the exponent (β) of the power law was determined (Fig. 6d). A β value of 1 is consistent with a persistent random walk while a β value of 2 indicates purely ballistic motion. The β value for clustered cells was 1.6 in the absence of an electric field. In contrast, the value of the exponent for isolated cells in the absence of an electric field was 1.03. These results demonstrate that in the absence of an external field, cell clustering provides supradiffusive and more ballistic character to cell movement.

The value of β increased with electric field strength, indicating that cells move in a less random path when biased by an electric field. Notably, the difference in the value of β between isolated cells and cell clusters remained fairly constant across all electric field strengths, thereby disentangling the effect of cell clustering and electric field on promoting ballistic cell movement. These results provide further evidence that the effects of cell clustering and the application of an electric field act additively, even if not entirely independently, on cell migration.

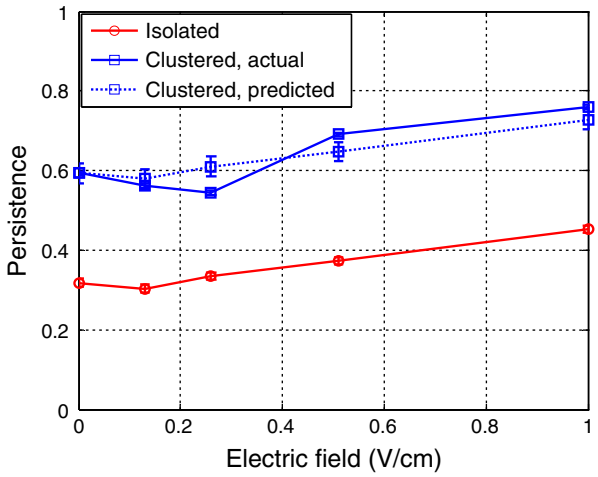

FIGURE 5. Persistence of cells under varying electric field strengths. The persistence was calculated as the ratio between net displacement and total distance traveled. The measured mean persistence (solid lines) for isolated (red) and clustered (blue) cells is shown for electric fields of 0, 0.13, 0.26, 0.51, and 1.0 V/cm. The predicted persistence for clustered cells (dotted blue) is calculated as the additive effect of the electric field and cell clustering (see "Materials and Methods"). Error bars for the measured persistence indicate standard error of the mean, and the error bars for the predicted persistence is computed by the propagation of errors of the measured values of persistence (see "Materials and Methods").

Clustered Cells Require Longer Time to Reorient in an Electric Field

Since clustered cells are slower and significantly more ballistic and persistent in their motion, even when no electric field is applied, we reasoned that cells in clusters may take longer to orient themselves within an electric field than isolated cells. To examine this hypothesis, we identified cells that were initially moving toward the cathode and quantified their reorientation toward the anode. Cells whose displacement was toward the cathode during the first hour were filtered, and their mean directedness was determined over time.

As shown in Fig. 7a, the directedness of filtered cells initially trends more negative as we are considering only cells that move toward the cathode. The directedness then recovers as these cells achieve their steady-state orientations. In the control case without an electric field, the directedness approaches a steady-state value near zero, as would be expected for all cells in the long term without any external bias. In the presence of an electric field, cells recover to a directedness value greater than that observed under control conditions. At higher electric fields, the directedness reaches a higher steady-state value. At extremely high potential (1 V/cm), an order of magnitude greater than the threshold needed to initiate electrotaxis (approx. 0.13 V/cm), both clustered and isolated cells achieve directedness in approximately the same timescale. This convergence suggests that cell–cell interactions may begin to break down at stronger electric fields. Except for the highest electric field, the directedness of isolated cells reaches a steady-state more quickly than that of clustered cells, consistent with our hypothesis.

To quantify the kinetics, the time course of the recovery in directedness was fit to an exponential function (Eq. (6)) by taking the nadir of the curve as the initial point and the characteristic time needed to reach half-maximal directedness was determined (Fig. 7b). The timescale for the reorientation of clustered cells was approximately 2–8 times longer than isolated cells in the absence of an electric field and for electric fields weaker than 1.0 V/cm. Since the difference in speed of isolated and clustered cells is only two-fold at all electric fields (Fig. 6c), the slower movement only partially explains the retarded reorientation kinetics of clustered cells. These results support our hypothesis that the inherent ballistic and persistent movement of clustered cells, is a significant contributing factor in the

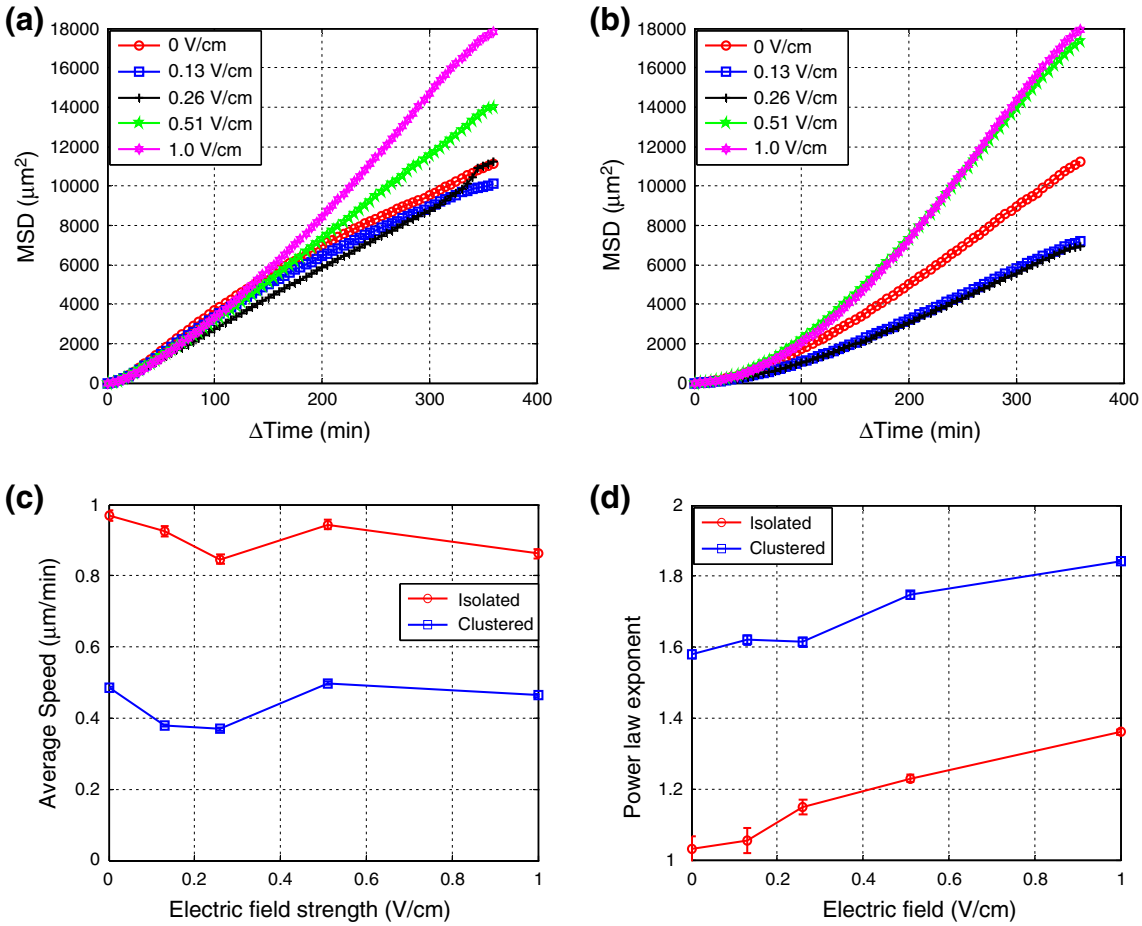

FIGURE 6. Mean square displacement of cells under varying electric field strengths. Mean square displacement (MSD) was calculated for (a) isolated cells and (b) clustered cells with time duration ranging from 0 to 6 h at 5 min intervals in the absence (red) or presence of electric field of 0.13 (blue), 0.26 (black), 0.51 (green), and 1.0 (magenta) V/cm. (c) Average speed of isolated (red) and clustered (blue) cells under varying electric field strengths. Cell speed is calculated as the path length of the cell divided by time. Error bars indicate standard error of the mean. (d) The MSD dependence on duration was fit to a power law and the corresponding exponent of the power law fit is shown for isolated (red) and clustered (cells) at electric fields of 0, 0.13, 0.26, 0.51, and 1.0 V/cm. Error bars represent 95% confidence intervals based on the power law fit.

slower orientation dynamics of clustered cells in electric fields of low to moderate magnitude.

DISCUSSION

In this study, we identify three significant features that distinguish the electrotaxis of clustered mammary epithelial cells from that of isolated cells. First, clustered cells are more sensitive to the magnitude of the electric potential than isolated cells: clustered cells achieve greater directedness at lower electric field strength. Second, cell clustering and an electric field have an approximately additive effect on the persistence of cell movement. Even in the absence of an external electric field, the migration trajectory of clustered cells is inherently more persistent than the random walk exhibited by isolated cells. The application of an electric field enhances this persistence but to a similar extent in both clustered and isolated cells, revealing that cell clustering and an electric field have separate, superimposable effects on the persistence of cell movement. Finally, we show that the inherent persistence of clustered cells renders them slower to align with an external electric field when compared to isolated cells. Thus, although clustered cells ultimately achieve a greater directedness at lower electric potential, the dynamics of their alignment are retarded by the extra time it takes to reorient cells that are already directed.

Clustered mammary epithelial cells align with an external electric field at a lower field strength than isolated cells. The effective potential (EP50) to reach half maximal fraction of aligned cells for clustered cells is approximately 0.2 V/cm whereas the EP50 for isolated cells is approximately 0.3 V/cm (Table 1). The

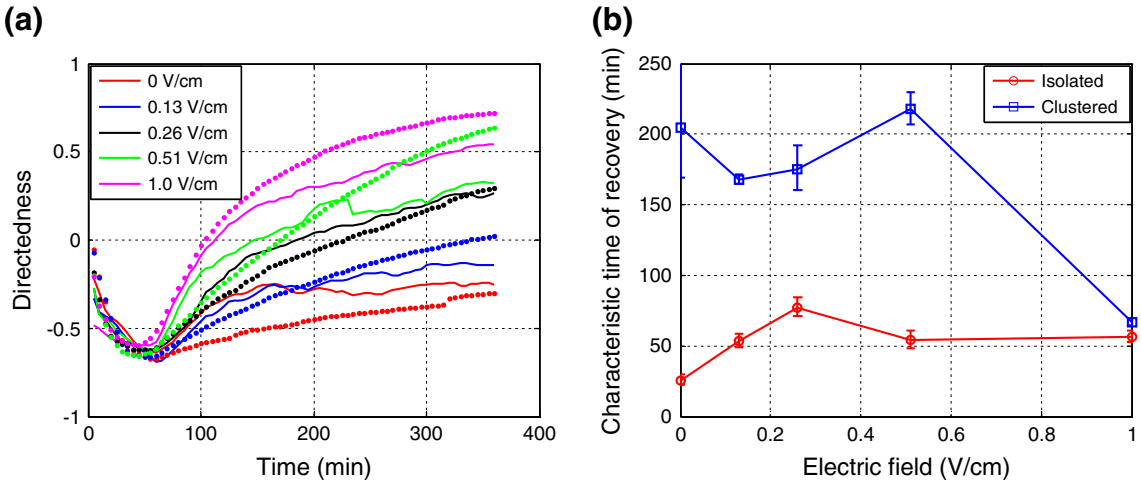

FIGURE 7. Dynamics of acquisition of electrotactic directedness by cells initially aligned opposite to the cathode–anode vector. (a) Directedness over time of isolated (solid lines) and clustered (dotted lines) cells which were initially moving toward the cathode and remained on such a trajectory for the duration of the first hour of observation is shown in the absence (red) or presence of electric field of 0.13 (blue), 0.26 (black), 0.51 (green), and 1.0 (magenta) V/cm (b) The characteristic time of recovery was calculated by fitting to an exponential recovery model and solving for the time required to reach half maximal directedness (see "Materials and Methods"). The characteristic time of recovery for isolated (red) and clustered (blue) cells is shown for electric fields of 0, 0.13, 0.26, 0.51, and 1.0 V/cm. Error bars represent 95% confidence intervals based on the exponential recovery model.

higher electrotactic sensitivity of clustered MCF-10A cells is consistent with observations that MDCK I and MDCK II cells are more sensitive to an electric field when clustered.[19] In comparison to MDCK cells, MCF-10A cells form weak tight junctions due to reduced expression of ZO-1,[10] leading us to conclude that strong tight junctions are not necessary for the enhanced electrotactic responsiveness of clustered cells. Meanwhile, E-cadherin-mediated adherens junctions seem to play an important role since the knockdown of E-cadherin abrogated the enhanced directedness of clustered MDCK cells in an electric field.[19]

Our data suggest that cell clusters align to an electric field with greater sensitivity than isolated cells because cells in clusters are inherently more directed. We find that even in the absence of an external field, the migration trajectory of clustered cells is highly persistent (Fig. 5) and comparatively ballistic (Fig. 6). In contrast, the migration paths of isolated cells exhibit diffusive behavior characterized by a linear dependence of mean square displacement (MSD) with time. Furthermore, exposure to an external electric field increases the persistence of both clustered and isolated cells in an equivalent manner. Since the electric field does not have a comparatively stronger effect on the persistence of clustered vs. isolated cells, we propose a model wherein the intrinsic persistence endowed by clustering underpins the enhanced sensitivity of clustered cells to an electric field.

At least two factors may contribute to the greater inherent persistence of cells in clusters. In the crowded environment of a cell cluster, a moving cell will collide with neighbors, thereby providing a non-stationary physical obstruction that constrains the direction in which neighbors can move. In addition to this physical obstruction, cell–cell adhesions provide the means for momentum transfer from one viscoelastic cell to another. Together, these mechanisms propagate the movement of one cell to bias neighboring cells, leading to collective directed movement greater than that observed in isolated cells. In the context of an electric field, a consequence of this inherent directedness is that aligning an individual cell in a cluster can have broader effects on its neighbors, thereby making the clustered population more responsive to an electric field than isolated cells. We are pursuing experimental and mathematical modeling approaches to examine these mechanisms in greater detail. Meanwhile, in this study, we focus on delineating further the implications of the intrinsic directedness of clustered cells on their electrotactic response.

Although the intrinsic directedness of clustered cells enables them to achieve greater directedness at lower electric potential, the kinetics to achieve alignment is 2–8 fold slower in clustered cells (Fig. 7). We examined cells that were moving away from the anode during the first hour and quantified how long it took them to redirect toward the anode. Clustered cells are 2–4 fold slower than isolated cells to achieve directedness to the anode. In addition, in the absence of an electric field, clustered cells are 8-fold slower to recover to a random distribution of orientations, demonstrating that the slower orientation kinetics is a property associated with the clustered state. While clustered cells move

two-fold slower than isolated cells (Fig. 6c), this disparity in migration speed only partially explains the 2–8 fold slower orientation dynamics of clustered cells. This analysis suggests that the inherent directedness of clustered cells is an additional significant factor in retarding the orientation dynamics.

Our findings have implications for our understanding of directed collective migration and for developing strategies to tune this physiologically significant mode of migration. Directed collective migration is a critical process in development and the progression of diseases, such as cancer.[4] In these contexts, external molecular fields, such as chemotactic or haptotactic gradients, play a prominent role in conferring directional bias.[7,34,38] It will be interesting to determine whether our finding that collective movement enhances sensitivity but retards the kinetics of alignment to an electric field extends to other external fields that bias cell movement. Meanwhile, the results from this study reveal that cell clustering leads to a trade-off in sensitivity vs. dynamics of electrotaxis. Our results provide deeper quantitative insights into this trade-off and help to define the operating space for technologies that seek to affect cell movement using electric fields in applications such as tissue engineering. In addition, electric fields are employed for reasons other than manipulating cell migration in a wide range of therapeutic applications, including drug delivery, hyperthermic eradication of tumors, spinal cord regrowth, and ulcer healing.[12,15,18,30] In such situations, our findings offer insights into the potential off-target effects of the external electric field on the migratory behavior of cells in the exposed region and the possible consequences for cellular organization of the tissue.

ELECTRONIC SUPPLEMENTARY MATERIAL

The online version of this article (doi: 10.1007/s12195-015-0383-x) contains supplementary material, which is available to authorized users.

ACKNOWLEDGMENTS

We thank the members of the Asthagiri group for helpful discussions. This work was supported by the National Institutes of Health grant R01CA138899 and start-up resources provided by Northeastern University.

CONFLICT OF INTEREST

Mark L. Lalli and Anand R. Asthagiri declare that they have no conflict of interest.

ETHICAL STANDARDS

No human or animal studies were carried out by the authors for this article.

REFERENCES

[1]Adams, D. S., and M. Levin. Endogenous voltage gradients as mediators of cell-cell communication: strategies for investigating bioelectrical signals during pattern formation. *Cell Tissue Res*. 352:95–122, 2013.
[2]Bai, H., C. D. McCaig, J. V. Forrester, and M. Zhao. DC electric fields induce distinct preangiogenic responses in microvascular and macrovascular cells. *Arterioscler. Thromb. Vasc. Biol*. 24:1234–1239, 2004.
[3]Berens, P. J. CircStat: a MATLAB toolbox for circular statistics. *Stat. Softw*. 31:1–21, 2009.
[4]Carey, S. P., A. Starchenko, A. L. McGregor, and C. A. Reinhart-King. Leading malignant cells initiate collective epithelial cell invasion in a three-dimensional heterotypic tumor spheroid model. *Clin. Exp. Metastasis* 30:615–630, 2013.
[5]Conant, C. G., J. T. Nevill, M. Schwartz, and C. Ionescu-Zanetti. Wound healing assays in well plate–coupled microfluidic devices with controlled parallel flow. *J. Assoc. Lab. Autom*. 15:52–57, 2010.
[6]Cuzick, J., R. Holland, V. Barth, R. Davies, M. Faupel, I. Fentiman, H. J. Frischbier, J. L. LaMarque, M. Merson, V. Sacchini, D. Vanel, and U. Veronesi. Electropotential measurements as a new diagnostic modality for breast cancer. *Lancet* 352:359–363, 1998.
[7]Debruyne, P. R., E. A. Bruyneel, I.-M. Karaguni, X. Li, G. Flatau, O. Müller, A. Zimber, C. Gespach, and M. M. Mareel. Bile acids stimulate invasion and haptotaxis in human colorectal cancer cells through activation of multiple oncogenic signaling pathways. *Oncogene* 21:6740–6750, 2002.
[8]Djamgoz, M. B. A., M. Mycielska, Z. Madeja, S. P. Fraser, and W. Korohoda. Directional movement of rat prostate cancer cells in direct-current electric field: involvement of voltage gated Na^+ channel activity. *J. Cell Sci*. 114:2697–2705, 2001.
[9]Einstein, A. Über die von der molekularkinetischen Theorie der Wärme geforderte Bewegung von in ruhenden Flüssigkeiten suspendierten Teilchen. *Ann. Phys*. 322:549–560, 1905.
[10]Fogg, V. C., C.-J. Liu, and B. Margolis. Multiple regions of Crumbs3 are required for tight junction formation in MCF10A cells. *J. Cell Sci*. 118:2859–2869, 2005.
[11]Foulds, A. T., and I. S. Barker. Human skin battery potentials and their possible role in wound healing. *Br. J. Dermatol* 109:515–522, 1983.
[12]Gibot, L., L. Wasungu, J. Teissié, and M.-P. Rols. Antitumor drug delivery in multicellular spheroids by electropermeabilization. *J. Control. Release* 167:138–147, 2013.
[13]Huang, C.-W., J.-Y. Cheng, M.-H. Yen, and T.-H. Young. Electrotaxis of lung cancer cells in a multiple-electric-field chip. *Biosens. Bioelectron*. 24:3510–3516, 2009.
[14]Kim, J.-H., L. J. Dooling, and A. R. Asthagiri. Intercellular mechanotransduction during multicellular morphodynamics. *J. R. Soc. Interface* 7:S341–S350, 2010.
[15]Kloth, L. C. Electrical stimulation for wound healing: a review of evidence from in vitro studies, animal

experiments, and clinical trials. *Int. J. Low. Extrem. Wounds* 4:23–44, 2005.
[16]Kushiro, K., and A. R. Asthagiri. Modular design of micropattern geometry achieves combinatorial enhancements in cell motility. *Langmuir* 28:4357–4362, 2012.
[17]Lamalice, L., F. Le Boeuf, and J. Huot. Endothelial cell migration during angiogenesis. *Circ. Res.* 100:782–794, 2007.
[18]Lehmann, K., A. Rickenbacher, J.-H. Jang, C. E. Oberkofler, R. Vonlanthen, L. von Boehmer, B. Humar, R. Graf, P. Gertsch, and P.-A. Clavien. New insight into hyperthermic intraperitoneal chemotherapy: induction of oxidative stress dramatically enhanced tumor killing in in vitro and in vivo models. *Ann. Surg.* 256:730–737; discussion 737–738, 2012.
[19]Li, L., R. Hartley, B. Reiss, Y. Sun, J. Pu, D. Wu, F. Lin, T. Hoang, S. Yamada, J. Jiang, and M. Zhao. E-cadherin plays an essential role in collective directional migration of large epithelial sheets. *Cell. Mol. Life Sci.* 69:2779–2789, 2012.
[20]Lin, F., F. Baldessari, T. Gyenge, C. Crenguta Sato, R. D. Chambers, J. G. Santiago, and E. C. Butcher, Lymphocyte electrotaxis in vitro and in vivo. *J. Immunol.* 181:2465–2471, 2008.
[21]Long, H., G. Yang, and Z. Wang. Galvanotactic migration of EA.Hy926 endothelial cells in a novel designed electric field bioreactor. *Cell Biochem. Biophys.* 61:481–491, 2011.
[22]Merks, R. M. H., E. D. Perryn, A. Shirinifard, and J. A. Glazier. Contact-inhibited chemotaxis in de novo and sprouting blood-vessel growth. *PLoS Comput. Biol.* 4:e1000163, 2008.
[23]Mycielska, M. E., and M. B. A. Djamgoz. Cellular mechanisms of direct-current electric field effects: galvanotaxis and metastatic disease. *J. Cell Sci.* 117:1631–1639, 2004.
[24]Ng, M. R., A. Besser, G. Danuser, and J. S. Brugge. Substrate stiffness regulates cadherin-dependent collective migration through myosin-II contractility. *J. Cell Biol.* 199:545–563, 2012.
[25]Patel, N., and M.-M. Poo. Orientation of neurite growth by extracellular electric fields. *J. Neurosci.* 2:483–496, 1982.
[26]Pu, J., C. D. McCaig, L. Cao, Z. Zhao, J. E. Segall, and M. Zhao. EGF receptor signalling is essential for electric-field-directed migration of breast cancer cells. *J. Cell Sci.* 120:3395–3403, 2007.
[27]Pu, J., and M. Zhao. Golgi polarization in a strong electric field. *J. Cell Sci.* 118:1117–1128, 2005.
[28]Riahi, R., Y. Yang, D. D. Zhang, and P. K. Wong. Advances in wound-healing assays for probing collective cell migration. *J. Lab. Autom.* 17:59–65, 2012.
[29]Rodriguez, L., and I. Schneider. Directed cell migration in multi-cue environments. *Integr. Biol.* 5:1306–1323, 2013.
[30]Shapiro, S. A review of oscillating field stimulation to treat human spinal cord injury. *World Neurosurg.* 81:830–835, 2012.
[31]Song, B., Y. Gu, J. Pu, B. Reid, Z. Zhao, and M. Zhao. Application of direct current electric fields to cells and tissues in vitro and modulation of wound electric field in vivo. *Nat. Protoc.* 2:1479–1489, 2007.
[32]Sun, Y.-S., S.-W. Peng, K.-H. Lin, and J.-Y. Cheng. Electrotaxis of lung cancer cells in ordered three-dimensional scaffolds. *Biomicrofluidics* 6:014102-1–014102-14, 2012.
[33]Sung, B. H., X. Zhu, I. Kaverina, and A. M. Weaver. Cortactin controls cell motility and lamellipodial dynamics by regulating ECM secretion. *Curr. Biol.* 21:1460–1469, 2011.
[34]Tao, Y., and M. Wang. Global solution for a chemotactic–haptotactic model of cancer invasion. *Nonlinearity* 21:2221–2238, 2008.
[35]Tsai, H.-F., S.-W. Peng, C.-Y. Wu, H.-F. Chang, and J.-Y. Cheng. Electrotaxis of oral squamous cell carcinoma cells in a multiple-electric-field chip with uniform flow field. *Biomicrofluidics* 6:034116-1–034116-12, 2012.
[36]van der Meer, A. D., K. Vermeul, A. A. Poot, J. Feijen, and I. Vermes. A microfluidic wound-healing assay for quantifying endothelial cell migration. *Am. J. Physiol. Heart Circ. Physiol.* 298:H719–H725, 2010.
[37]Vedula, S. R. K., M. C. Leong, T. L. Lai, P. Hersen, A. J. Kabla, C. T. Lim, and B. Ladoux. Emerging modes of collective cell migration induced by geometrical constraints. *Proc. Natl. Acad. Sci. U.S.A.* 109:12974–12979, 2012.
[38]Wang, S.-J., W. Saadi, F. Lin, C. M. Nguyen, and N. L. Jeon. Differential effects of EGF gradient profiles on MDA-MB-231 breast cancer cell chemotaxis. *Exp. Cell Res.* 300:180–189, 2004.
[39]Wang, E., M. Zhao, J. V. Forrester, and C. D. MCCaig. Re-orientation and faster, directed migration of lens epithelial cells in a physiological electric field. *Exp. Eye Res.* 71:91–98, 2000.
[40]Zhao, M., B. Song, J. Pu, T. Wada, B. Reid, G. Tai, F. Wang, A. Guo, P. Walczysko, Y. Gu, T. Sasaki, A. Suzuki, J. V. Forrester, H. R. Bourne, P. N. Devreotes, C. D. McCaig, and J. M. Penninger. Electrical signals control wound healing through phosphatidylinositol-3-OH kinase-gamma and PTEN. *Nature* 442:457–460, 2006.
[41]Zhao, M. Electrical fields in wound healing-An overriding signal that directs cell migration. *Semin. Cell Dev. Biol.* 20:674–682, 2009.